Cavity-Assisted Quantum Bath Engineering

K. W. Murch, U. Vool, D. Zhou, S. J. Weber, S. M. Girvin, and I. Siddiqi

Phys. Rev. Lett. **109**, 183602 — Published 31 October 2012

DOI: 10.1103/PhysRevLett.109.183602

Cavity-assisted quantum bath engineering

K. W. Murch*,[1] U. Vool,[2] D. Zhou,[2] S. J. Weber,[1] S.M. Girvin,[2] and I. Siddiqi[1]

[1] *Quantum Nanoelectronics Laboratory, Department of Physics, University of California, Berkeley CA 94720*
[2] *Department of Physics, Yale University, New Haven, CT 06520-8120*

(Dated: September 17, 2012)

We demonstrate quantum bath engineering for a superconducting artificial atom coupled to a microwave cavity. By tailoring the spectrum of microwave photon shot noise in the cavity, we create a dissipative environment that autonomously relaxes the atom to an arbitrarily specified coherent superposition of the ground and excited states. In the presence of background thermal excitations, this mechanism increases the state purity and effectively cools the dressed atom state to a low temperature.

PACS numbers:

In practice, quantum systems are never completely isolated, but instead interact with degrees of freedom in the surrounding environment, eventually leading to decoherence of some states of the system. Precision measurement techniques such as nuclear magnetic resonance and interferometry, as well as envisioned quantum schemes for computation, simulation, and data encryption, rely on the ability to prepare and preserve delicate quantum superpositions and entanglement. The conventional route to long-lived quantum coherence involves minimizing coupling to a dissipative bath. Paradoxically, it is possible to instead engineer specific couplings to a quantum environment that allow dissipation to actually preserve coherence[1–3]. In this letter, we demonstrate such quantum bath engineering for a superconducting artificial atom coupled to a microwave frequency cavity. Cavity-assisted cooling of the atom is tailored to produce any arbitrary superposition of ground and excited states on demand with high fidelity.

The concept of our experiment is shown in Figure 1. A two-level atom is driven resonantly at frequency ω_q. In the frame rotating at the drive frequency, the two eigenstates of the system are $|\pm\rangle = (|g\rangle \pm |e\rangle)/\sqrt{2}$, with eigenvalues ± 1 of the σ_x Pauli operator. The energy splitting between the $|+\rangle$ and $|-\rangle$ states is given by the Rabi frequency, Ω_R. If $\hbar\Omega_R \ll k_B T_{eff}$, where T_{eff} is the effective temperature, neither state is thermodynamically preferred. However, by weakly coupling the atom to a cavity and introducing an additional drive detuned from the cavity resonance by $\Delta_c = \omega_d - \omega_c$, the photon shot noise of the cavity forms a quantum bath for the atom which can be engineered such that dissipation drives the atom to the $|+\rangle$ or $|-\rangle$ state. Here, $\omega_d(\omega_c)$ is the drive (cavity resonance) frequency. For red detuned drive, $(\Delta_c < 0)$, the cavity dissipation "cools" the atom to the $|+\rangle$ state.

Cavity assisted cooling has been studied extensively in the context of atomic gases[4–7], mechanical objects[8–11] and spins[12]. Similarly, single atoms and qubits have been used to alter the dissipation environment of a resonator, leading to lasing[13,14], cooling, and amplification[15–17]. We demonstrate that cavity cooling can be applied to the dressed states of a two-level atom, and the dissipation introduced by the drive may be engineered to relax the system towards any specified point on the Bloch sphere—a valuable resource in quantum information processing. This process is resonant and can produce large cooling rates.

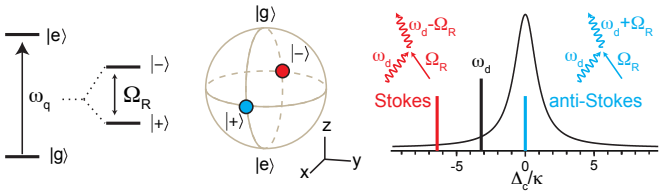

FIG. 1: Cavity cooling of a dressed state. A two-level atom is driven resonantly to form new eigenstates, $|+\rangle$ and $|-\rangle$ in the rotating frame. Driving the cavity at $\Delta_c = -\Omega_R$ resonantly enhances the anti-Stokes process relaxing the system to the $|+\rangle$ state.

Our two-level atom is realized using the two lowest energy levels of a superconducting transmon qubit[18,19] with $\omega_q/2\pi = 5.0258$ GHz, dispersively coupled to the TE_{101} mode of a 3D superconducting cavity with frequency $\omega_c/2\pi = 6.826$ GHz and linewidth $\kappa/2\pi = 4.3$ MHz. The qubit induces a state-dependent frequency shift on the cavity of $-\chi\sigma_z$ where $\chi/2\pi = -0.66$ MHz is the dispersive coupling strength. Similarly, the qubit frequency undergoes a light (or AC Stark) shift depending on the intracavity photon number, $\hat{n}$, with mean value denoted $\omega_q' = \omega_q + 2\chi\bar{n}$. The Hamiltonian for the qubit in the frame rotating at ω_q is,

$$H = -\frac{\Omega_R}{2}\sigma_x - \chi a^\dagger a \sigma_z, \qquad (1)$$

where $a^\dagger(a)$ is the cavity photon creation (annihilation) operator. Transition rates between the $|+\rangle$ and $|-\rangle$ states are determined from Redfield theory[20], $\Gamma_\pm = [4\chi^2 S_{nn}(\mp\Omega_R) + \tilde{S}_{yy}(\mp\Omega_R) + \tilde{S}'_{zz}(\mp\Omega_R)]/4$, where $\tilde{S}_{yy} \simeq 1/(T_1)$ and $\tilde{S}'_{zz} \simeq 2/(T_\varphi)$ are the power spectral densities of noise orthogonal to the x axis in the rotating frame, and $S_{nn}(\omega) = \bar{n}\kappa[(\kappa/2)^2 + (\omega+\Delta_c)^2]^{-1}$ is the spectral density of photon number fluctuations in the cavity[20]

that characterize the quantum bath. T_1 and T_φ are the energy decay and pure dephasing times for the qubit, respectively. For $\Delta_c = 0$, S_{nn} is symmetric in frequency and corresponds to an infinite temperature bath. In this case S_{nn} causes dephasing of the qubit and can equivalently be described in terms of a fluctuating AC stark shift, or in terms of measurement induced dephasing[20,21]. When $\Delta_c \neq 0$, S_{nn} is asymmetric and corresponds to a bath with finite positive (or negative) temperature and can be used to cool (or invert) the qubit state[20]. As illustrated in Figure 1, cooling takes place via inelastic Raman scattering of pump photons. The most efficient cooling to the $|+\rangle$ state takes place for $\Delta_c = -\Omega_R$ where the anti-Stokes photons are on resonance with the cavity. At this point the net cooling and heating rates are,

$$\Gamma_- = \frac{4\chi^2\bar{n}}{\kappa} + \frac{1}{2T_2}, \quad \Gamma_+ = \frac{\kappa\chi^2\bar{n}}{(2\Omega_R)^2 + (\kappa/2)^2} + \frac{1}{2T_2}, \quad (2)$$

respectively, where $T_2 = (1/2T_1 + 1/T_\varphi)^{-1} = 10.6$ μs is the (lab frame) dephasing rate. In equilibrium with the cavity bath, the final qubit polarization is given by detailed balance.

The state of the qubit was probed by measuring the phase shift of a microwave tone reflecting off of the cavity at the cavity resonance frequency. The reflected signal was amplified by a lumped-element Josephson parametric amplifier (LJPA) operating in phase sensitive mode which allowed high fidelity, multi-state, single shot readout of the qubit state. Our qubit sample exhibited excited (and higher excited) state population in excess of what would be expected from the nominal $T = 20$ mK environment. For our measurements, we used post selection to disregard the higher excited state populations which was as much as 12% of the qubit population.

To demonstrate effective quantum bath engineering, we compare a Ramsey measurement (Fig. 2(a)), to an experiment in which the qubit was cooled to the $|+\rangle$ state. The Ramsey measurement consisted of two $\pi/2$ pulses detuned by 2.8 MHz from the qubit frequency, followed by state readout in the σ_z basis and showed a typical $T_2^* = 4.9$ μs exponential decay of coherence. In Figure 2(b), the cavity was driven to cool the qubit to the $|+\rangle$ state. After cooling the state for a variable period of time, the remaining coherence was measured by applying a $\pi/2$ pulse at a frequency detuned by 2.8 MHz from ω_q' and measuring the amplitude of the resulting oscillations in the ground state population. We note that there is an initial build up of the coherence over a time scale of less than 1 μs given by $\Gamma^{-1} = (\Gamma_+ + \Gamma_-)^{-1}$ after which the system enters a steady state and the coherent oscillations persist indefinitely.

In Figure 3 we present tomography of the qubit state after it has come to equilibrium with the dissipative environment presented by the cavity. The qubit was driven at a variable detuning $\Delta_q = \omega_q - \omega_r$, where ω_r is the drive frequency, and at variable cavity drive power detuned from the cavity by $\Delta_c/2\pi = -9$ MHz. The amplitude of the qubit drive was fixed to give $\Omega_R/2\pi = +9$ MHz on resonance. In Figure 3(a) we display the tomography data for $\langle\sigma_x\rangle$ and $\langle\sigma_z\rangle$ (note that in the rotating frame $\langle\sigma_y\rangle = 0$). The dashed line indicates the dependence of $\omega_q - \omega_q'$ on the drive power, P_d, indicating the detuning where the drive maintains resonance with the light-shifted qubit. Following this curve, we plot $\langle\sigma_x\rangle$ and $\langle\sigma_z\rangle$ as a function of cavity photon number in Figure 3(b). When $\bar{n} = 0$, $\Gamma_+ = \Gamma_- = 1/(2T_2)$ and the system is completely incoherent. As the number of intracavity photons increases, coherence builds up along the x direction and saturates around $\bar{n} = 1$. The purity of the cooled state is given by $\Gamma_-/(\Gamma_+ + \Gamma_-)$. The observed maximum state purity was 70% and was limited by our state readout fidelity ($\sim 90\%$) and population relaxation to the second excited state of the transmon. The latter reduced the measured state purity by up to an additional $\sim 20\%$ depending on the time delay between the tomography pulses and the readout. The combination of these two effects led to a 70-80% reduction in the measured state purity. Taking into account these reductions, our measurements are close to the predicted value, plotted as a dashed line in Figure 3(b).

When $|\chi\sqrt{\bar{n}}| > \kappa$, the system is in a regime of strong coupling where higher-order and rapidly-rotating terms that have so far been neglected become significant. To explore this regime, we performed numerical simulations of the master equation. These results are shown in Figure 3(b) as solid blue and gray lines and indicate that the maximum state purity is reduced compared to the predictions of Eq. (2) at high drive powers. Based on the simulation, we estimate that the *actual* state purity was 94%, which corresponds to an effective temperature in

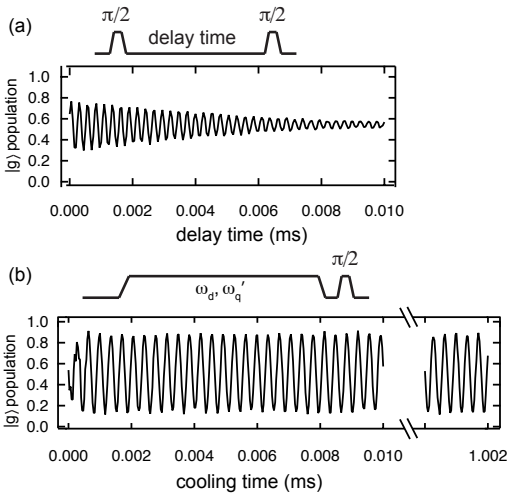

FIG. 2: (a) Ramsey measurement using detuned pulses. (b) Cavity cooling to the $|+\rangle$ state with $-\Delta_c/2\pi = \Omega_R/2\pi = 9$ MHz, and $\bar{n} = 3.6$. After driving the system at ω_q' and ω_d for a variable time, a detuned $\pi/2$ pulse transfers the remaining coherence to the σ_z basis. High contrast, persistent "Ramsey" fringes indicate that the qubit has been cooled to the $|+\rangle$ state.

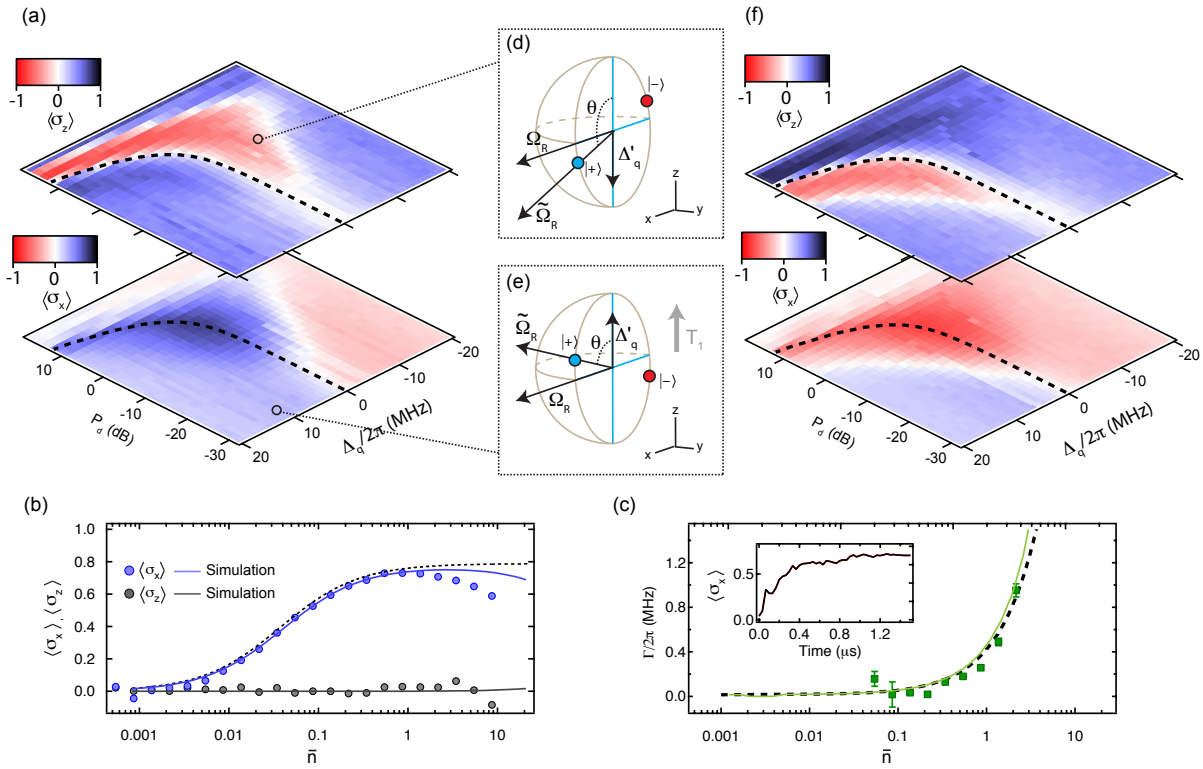

FIG. 3: **State tomography.** (a) Color plots show $\langle\sigma_x\rangle$ and $\langle\sigma_z\rangle$ as a function of cavity drive power ($P_d = 10\log(\bar{n})$ (dB)) and qubit drive detuning for fixed cavity drive detuning, $-\Delta_c/2\pi = \Omega_R/2\pi = 9$ MHz. The dashed line indicates the optimal detuning $\Delta'_q = \omega'_q - \omega_r = 0$. (b,c) $\langle\sigma_x\rangle$, $\langle\sigma_z\rangle$ and the cooling rate are plotted versus $\bar{n}$ for $\omega_r = \omega'_q$. The dashed lines indicates the prediction from Eq. (2) which has been scaled by our measurement fidelity of 80%.The solid blue, gray, and green lines indicate the results of the simulations for $\langle\sigma_x\rangle$, $\langle\sigma_z\rangle$ and the cooling rate respectively. Error bars in (c) represent the estimated error in the exponential fit. (inset in c) $\langle\sigma_x\rangle$ vs. cooling time for $\bar{n} = 1.4$. (d,e) Bloch sphere diagrams indicate that when the qubit drive is off resonance, the $|\pm\rangle$ states are tilted from the equator of the Bloch sphere. (f) Color plot shows inversion of $\langle\sigma_x\rangle$ and $\langle\sigma_z\rangle$ for $+\Delta_c/2\pi = \Omega_R/2\pi = 9$ MHz.

the rotating frame of $T_{\rm eff} = 150$ μK for the dressed state.

To quantify the strength of the cavity damping, we plot the measured cooling rate in Figure 3(c), obtained by measuring the exponential timescale for buildup of ensemble population in the $|+\rangle$ state as the duration of the cooling pulse was increased (Fig. 3(c), inset). The measured rate is in quantitative agreement with Eq. (2), shown as a dashed line, as long as $|\chi\sqrt{\bar{n}}| < \kappa$. At higher photon numbers, the observed increase in coherence was not exponential. In this regime, the system is expected to exhibit damped oscillations between $|-\rangle$ and $|+\rangle$ in analogy with vacuum Rabi oscillations (see the supplementary information).

When the qubit drive is off-resonant, the engineered dissipation drives the qubit to different points on the Bloch sphere. As we illustrate in Figure 3(d), the off-resonant qubit drive creates an effective magnetic field at an angle $\theta = \arctan(\Omega_R/\Delta'_q)$ with respect to the z axis, tilting the $|\pm\rangle$ states from the equator of the Bloch sphere. Here, $\Delta'_q = \omega'_q - \omega_r$ is the detuning of the AC stark shifted qubit frequency from the qubit drive. In this case the cavity dissipation drives the system to the state obeying $\sigma_\theta|+\rangle = (+1)|+\rangle$ where $\sigma_\theta \equiv \sin\theta\sigma_x + \cos\theta\sigma_z$. When the cavity drive is very weak (Fig. 3(e)) dissipation due to the finite qubit $T_1 = 10$ μs favors the $|-\rangle$ state when $\Delta'_q > 0$. In Figure 3(f) we display qubit state tomography when the cavity drive detuning, $+\Delta_c/2\pi = \Omega_R/2\pi = 9$ MHz. In this case the cavity dissipation inverts the qubit to the $|-\rangle$ state.

By driving the qubit off-resonance and altering the cavity detuning to remain equal to the off-resonant Rabi frequency, $\tilde{\Omega}_R = \sqrt{\Omega_R^2 + \Delta'^2_q}$, arbitrary superposition states of $|g\rangle$ and $|e\rangle$ can be prepared using the cavity dissipation. As we show in the supplemental information, the heating and cooling rates are reduced by $(\Omega_R/\Delta'_q)^2$ since the qubit drive is no longer resonant. In Figure 4 we display measurements that demonstrate cooling to arbitrary latitudes on the Bloch sphere. Figure 4 displays $\langle\sigma_\theta\rangle$ for $\theta = \{90°, 43°, 10°\}$ for $\Delta_c/2\pi = -15$ MHz and variable drive power and detuning. For $\theta = \pi/2$ the cooling is along x as in Figure 3(a). As θ is decreased (Fig. 4(b-c)), the optimum cooling occurs for $\Delta'_q = \sqrt{\Delta_c^2 - \Omega_R^2}$.

For a weak Rabi drive strongly detuned from ω'_q, θ approaches zero, $|+\rangle \simeq |g\rangle$, and the cavity dissipation mech-

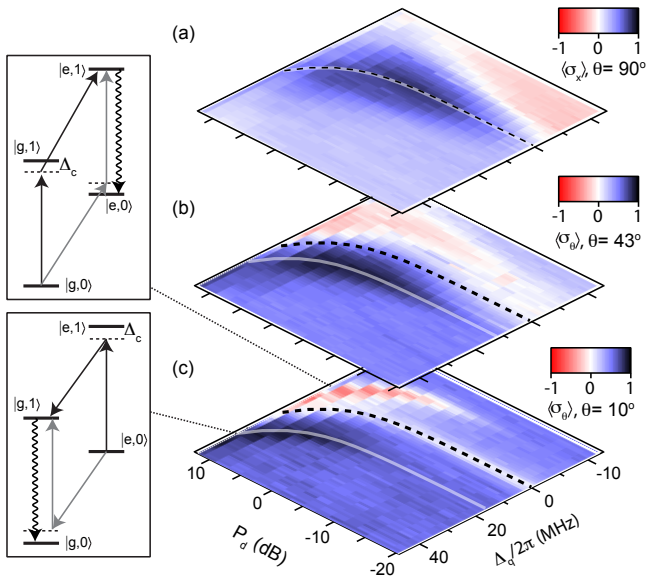

FIG. 4: **Preparing arbitrary superposition states using cavity dissipation.** Measurements of $\langle\sigma_\theta\rangle$ where $\sigma_\theta \equiv \sin\theta\sigma_x + \cos\theta\sigma_z$ for $\theta = \{90°, 43°, 10°\}$, (a-c), versus drive power and qubit-drive detuning. The dashed lines indicate $\omega_q' - \omega_q$. The transparent gray lines indicate the qubit drive detuning that gives the most efficient cooling, $(\Delta_c^2 - \Omega_R^2)^{1/2}$. For $\theta = 10°$, two sideband transitions are visible corresponding to Raman transitions that leave the qubit in the ground (lower inset) or excited state (upper inset). The ground state Raman process (lower inset) involves absorption of a cavity drive photon, stimulated emission at $\omega_q' + \Delta_c$, and emission into the cavity at ω_c. Two possible processes are labeled by gray and black arrows.

anism crosses over to ordinary cavity-assisted Raman sideband cooling transitions similar to the transitions used to cool atoms[22–25] and superconducting qubits[26] using a strong atomic transition to enhance emission at a specific frequency. Here, the cavity takes the place of the strong atomic transition. In Figure 4(c), with $\theta = 10°$, two "sideband" transitions emerge for $P_d > 0$ dB. Level diagrams of the transitions are shown as insets in Figure 4 indicating that simultaneously detuning the drives from the cavity and qubit allows selective optical pumping from the ground or excited states. The rates for these transitions can be calculated using Fermi's golden rule and agree with a calculation based on Redfield theory (see the supplementary information).

As we previously noted, when $\Delta_c = 0$, photon number fluctuations induce dephasing of the qubit in accordance with the theory of quantum measurement[20]. In this regime, cavity photons convey information about the qubit state encoded as a phase shift corresponding to an elastic scattering event. When the drive is detuned, the measurement is replaced by an inelastic scattering process in which the scattering of a photon into the cavity heralds a transition to the effective ground state of the system.

In conclusion, we have demonstrated quantum bath engineering with a model two-level system. The technique allows arbitrary superposition states of the the system to be prepared simply with saturating pulses. In contrast to measurement based feedback[27–30], the technique is a form of coherent quantum feedback[31,32] and is not limited by the quantum measurement efficiency. State preparation fidelities in excess of 99.9% are in principle possible with currently achievable sample parameters ($T_2 = 150$ μs, $\kappa/2\pi = 2$ MHz, $\Omega_R/2\pi = 50$ MHz, $\chi/2\pi = -1$ MHz). Future multi-qubit implementations could enable the preparation of entangled many-body states suitable for quantum simulation and computation.

We thank R. Vijay for contributions to the LJPA and helpful comments. This research was supported in part by the National Science Foundation (DMR-1004406), the U.S. Army Research Office (W911NF-11-1-0029 and W911NF-09-1-0514) and the Office of the Director of National Intelligence (ODNI), Intelligence Advanced Research Projects Activity (IARPA), through the Army Research Office. All statements of fact, opinion or conclusions contained herein are those of the authors and should not be construed as representing the official views or policies of IARPA, the ODNI, or the US Government.

[1] J. F. Poyatos, J. I. Cirac, and P. Zoller, Phys. Rev. Lett. **77**, 4728 (1996).
[2] B. Kraus, H. P. Büchler, S. Diehl, A. Kantian, A. Micheli, and P. Zoller, Phys. Rev. A **78**, 042307 (2008).
[3] D. Marcos, V. Tomadin, S. Diehl, and P. Rabl, New J. Phys. **14**, 055005 (2012).
[4] P. Horak, G. Hechenblaikner, K. M. Gheri, H. Stecher, and H. Ritsch, Phys. Rev. Lett. **79**, 4974 (1997).
[5] V. Vuletić and S. Chu, Phys. Rev. Lett. **84**, 3787 (2000).
[6] P. Maunz, T. Puppe, I. Schuster, N. Syassen, and G. Rempe, Nature **428**, 50 (2004).
[7] D. R. Leibrandt, J. Labaziewicz, V. Vuletić, and I. L. Chuang, Phys. Rev. Lett. **103**, 103001 (2009).
[8] O. Arcizet, P. Cohadon, T. Briant, M. Pinard, and A. Heidmann, Nature **444**, 71 (2006).
[9] S. Gigan, H. R. Bohm, P. M., F. Blaser, G. Langer, H. J. B., S. K. C., D. Bauerle, A. M., and A. Zeilinger, Nature **444**, 67 (2006).
[10] A. Naik, O. Buu, M. D. LaHaye, A. D. Armour, A. A. Clerk, M. P. Blencowe, and K. C. Schwab, Nature **443**, 193 (2006).
[11] A. Schliesser, P. DelHaye, N. Nooshi, K. J. Vahala, and T. J. Kippenberg. T. , Phys. Rev. Lett. **97**, 243905 (2006).
[12] N. Brahms and D. M. Stamper-Kurn, Phys. Rev. A **82**, 041804 (2010).
[13] J. McKeever et al., Nature **425**, 268 (2003).
[14] J. Hauss, A. Fedorov, C. Hutter, A. Shnirman, and G. Schön, Phys. Rev. Lett. **100**, 037003 (2008).
[15] E. Il'ichev, N. Oukhanski, A. Izmalkov, T. Wagner, M. Grajcar, H.-G. Meyer, A. Y. Smirnov, A. Maassen van den Brink, M. H. S. Amin, and A. M. Zagoskin, Phys. Rev. Lett. **91**, 097906 (2003).
[16] M. Grajcar, S. H. W. V. D. Ploeg, A. Izmalkov, E. Il'ichev, H. G. Meyer, A. Fedorov, A. Shnirman, and G. Schön, Nature Physics **4**, 612 (2008).
[17] G. Oelsner, P. Macha, O. Astafiev, E. Ilichev, M. Grajcar, U. Hübner, B. Ivanov, P. Neilinger, , and H.-G. Meyer, arXiv:1205.3017 (2012).
[18] J. Koch, T. M. Yu, J. Gambetta, A. A. Houck, D. I. Schuster, J. Majer, A. Blais, M. H. Devoret, S. M. Girvin, and R. J. Schoelkopf, Phys. Rev. A **76**, 042319 (2007).
[19] H. Paik, D. I. Schuster, L. S. Bishop, G. Kirchmair, G. Catelani, A. P. Sears, B. R. Johnson, M. J. Reagor, L. Frunzio, L. I. Glazman, et al., Phys. Rev. Lett. **107**, 240501 (2011).
[20] A. A. Clerk, M. H. Devoret, S. M. Girvin, F. Marquardt, and R. J. Schoelkopf, Rev. Mod. Phys. **82**, 1155 (2010).
[21] M. Boissonneault, J. M. Gambetta, and A. Blais, Phys. Rev. A **79**, 013819 (2009).
[22] D. J. Wineland and W. M. Itano, Phys. Rev. A **20**, 1521 (1979).
[23] W. Neuhauser, M. Hohenstatt, P. Toschek, and H. Dehmelt, Phys. Rev. Lett. **41**, 233 (1978).
[24] F. Diedrich, J. C. Bergquist, W. M. Itano, and D. J. Wineland, Phys. Rev. Lett. **62**, 403 (1989).
[25] S. E. Hamann, D. L. Haycock, G. Klose, P. H. Pax, I. H. Deutsch, and P. S. Jessen, Phys. Rev. Lett. **80**, 4149 (1998).
[26] S. O. Valenzuela, W. D. Oliver, D. M. Berns, K. K. Berggren, L. S. Levitov, and T. P. Orlando, Science **314**, 1589 (2006).
[27] J. Wang and H. M. Wiseman, Phys. Rev. A **64**, 063810 (2001).
[28] H. F. Hofmann, G. Mahler, and O. Hess, Phys. Rev. A **57**, 4877 (1998).
[29] A. N. Korotkov, Phys. Rev. B **63**, 115403 (2001).
[30] C. Sayrin, I. Dotsenko, X. Zhou, B. Peaudecerf, T. Rybarczyk, S. Gleyzes, P. Rouchon, M. Mirrahimi, H. Amini, M. Brune, et al., Nature **477**, 73 (2011).
[31] S. Lloyd, Phys. Rev. A **62**, 022108 (2000).
[32] H. Mabuchi, Phys. Rev. A **78**, 032323 (2008).